JOURNAL OF SYNCHROTRON RADIATION

ISSN 1600-5775

Controlling X-ray deformable mirrors during inspection

Lei Huang,[a]* Junpeng Xue[a,b] and Mourad Idir[a]

[a]NSLS-II, Brookhaven National Laboratory, Bldg 703, Upton, NY 11973-5000, USA, and [b]Sichuan University, People's Republic of China. *Correspondence e-mail: huanglei0114@gmail.com

Received 19 July 2016
Accepted 14 September 2016

Edited by S. Svensson, Uppsala University, Sweden

Keywords: X-ray deformable mirror; active optics; mirror inspection; windowed Fourier transform; B-spline curve fitting.

The X-ray deformable mirror (XDM) is becoming widely used in the present synchrotron/free-electron laser facilities because of its flexibility in correcting wavefront errors or modification of the beam size at the sample location. Owing to coupling among the N actuators of an XDM, $(N + 1)$ or $(2N + 1)$ scans are required to learn the response of each actuator one by one. When the mirror has an important number of actuators (N) and the actuator response time including stabilization or the necessary metrology time is long, the learning process can be time consuming. In this work, a fast and accurate method is presented to drive an XDM to a target shape usually with only three or four measurements during inspection. The metrology data are used as feedback to calculate the curvature discrepancy between the current and the target shapes. Three different derivative estimation methods are introduced to calculate the curvature from measured data. The mirror shape is becoming close to the target through iterative compensations. The feasibility of this simple and effective approach is demonstrated by a series of experiments.

1. Introduction

The use of adaptive optics or deformable mirrors (DMs) has been extensively studied for the compensation of wavefront distortion in various applications in the visible-light domain including human vision, space applications, optical communications, lasers and microscopy (Tyson, 2000). After years of improvement from a theoretical concept, to the early experimental stage, and finally turning into a sort of standard X-ray optics tool, nowadays the X-ray deformable mirror (XDM) is widely utilized at many synchrotron/free-electron laser light sources (Idir & Mercere, 2013). The XDM is now becoming an integral part not only in the present but also in the future large X-ray and EUV projects and will be essential in utilizing the full potential of new light sources currently under construction. The primary objective of using an XDM in a synchrotron radiation or a free-electron laser facility is to correct wavefront errors or enable variable focus beam sizes for different experimental setups, which are important aspects of the performance and flexibility of a beamline.

XDMs are usually long silicon (or glass) mirrors used at grazing incidence and equipped with N voltage-controlled actuators allowing local shape deformations. In order to exploit the full potential of an XDM, it is commonly necessary to perform a calibration or learning process to drive the mirror to the desired target shape. Usually, in order to optimize the voltages on actuators for minimized slope or height errors, the characterization of the XDM is carried out using the following process: an initial measurement needs to be collected, for example with all voltages of actuators set as 0 V, and N or $2N$

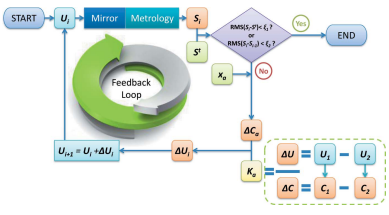

measurements are then taken to extract the influence function. The influence function is the characteristic of an XDM corresponding shape response to the action of a single actuator. In the classical learning process of an XDM, $(N + 1)$ or $(2N + 1)$ measures are required in total to obtain all actuators' influence function. However, when the number of the actuators N is relatively large, *e.g.* $N = 16$, and the actuator response or the necessary metrology is slow, *e.g.* 1 h, then the learning process can be time consuming, which is neither expected nor preferred for the day-to-day mirror inspection in a metrology laboratory.

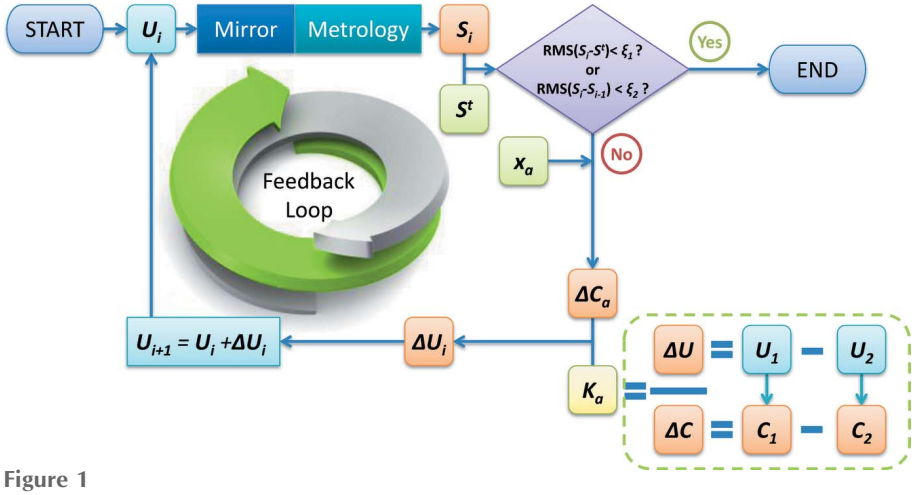

Figure 1
A feedback loop minimizes the shape error from the target.

In this work, we present a fast and accurate method to drive an X-ray active bimorph mirror to the desired target shape usually with only three or four measurements during mirror inspection. Instead of sequentially measuring and calculating the influence function of each actuator and then predicting the voltages, the metrology data are directly used to 'guide' the XDM from its current status towards the particular target *via* iterative compensations. The feedback in the iteration process is the curvature error at each actuator location from the desired target. The curvature is estimated from the measured slope or height data through derivative calculation. Three methods are introduced to estimate the derivative from the measured data. The paper is organized as follows. §2 introduces the principle of the proposed method; the experimental results are described in §3, and section §4 discusses some potential improvements.

2. Principle

In the adaptive optics community, the measurement of the influence function plays a vital role in assessing the performance of a DM. As one of the most important parameters of a DM, the influence function determines its achievable correction capability. Measuring the influence function (learning process) can be very fast for classical adaptive optics used in visible light (astronomy, laser, *etc.*). However, in the X-ray domain, mirror metrology is often performed using a slope or height profiler and the measuring time can be as long as 1 h for a 500 mm-long mirror.

Unlike the classical learning process generally used for adaptive optics (Tyson, 2000; Vannoni *et al.*, 2015, 2016), the proposed approach does not sequentially measure the influence functions but utilizes the metrology data to guide the XDM towards the target shape with a closed-loop feedback mechanism. The essential principle is to generate voltage feedback *via* the curvature estimation from the metrology data. In order to achieve the minimal shape difference from the target, voltages applied to the actuators are adjusted until the minimization goal is achieved. Fig. 1 illustrates a flow chart of the whole procedure with a feedback loop.

The starting voltages could be any applicable values. The initial voltages for the actuators are usually set to the suggested values either from XDM fabricator or by simulations, or even just simply set as zero volts. The XDM under the present voltages is then measured with a slope- or height-measurement instrument, *e.g.* NOM/LTP (Qian *et al.*, 1995; Takacs *et al.*, 1987; Siewert *et al.*, 2004) or an interferometer (Yamauchi *et al.*, 2003). In Fig. 1, the symbol S^t stands for the target shape, which can be the slope or height depending on the metrology tool, and S_i is the shape measurement result in the ith iteration. If the root mean square (RMS) of the shape error $S_i - S^t$ is under the specified value ξ_1 or the shape update $S_i - S_{i-1}$ is within the measurement uncertainty ξ_2 of the metrology instrument, then the iteration stops. Otherwise, the loop continues by calculating voltage updates. The curvature difference ΔC_a at each actuator location compared with the target is estimated after comparing the difference between the current and the target shape. Applying the hypothesis that there is the same linear-dependent voltage–curvature relationship of all actuators, see equation (1), the voltage feedback ΔU can be calculated,

$$\Delta U = K\,\Delta C, \tag{1}$$

where the coefficient K links the necessary voltages to have a curvature change on the mirror. The value of K can be sometimes provided by the XDM fabricator or experimentally determined by calculating the changes of curvature from two measurements with different input voltages. Once the voltage feedback ΔU for each actuator is determined, a new set of voltages $U_{i+1} = U_i + \Delta U_i$ can be updated to close the loop as illustrated in Fig. 1 and the next iteration begins with applying the new voltages to the XDM for measurement.

The measurement data from metrology instruments are commonly the slope or height, not directly the curvature, so it is necessary to estimate the curvature from the measured slope dz/dx or height z. The curvature can be expressed as

$$C = \frac{d^2z/dx^2}{\left[1 + (dz/dx)^2\right]^{3/2}}. \quad (2)$$

Since the slope of the X-ray mirror dz/dx is usually rather small compared with unity, the curvature can be expressed as the first derivative of the slope, *i.e.* the second derivative of the height, as described by

$$C \approx d^2z/dx^2. \quad (3)$$

Once the first derivative has been accurately estimated, it is straightforward to push it to the second derivative; therefore in this work we focus on curvature estimation from the measured slope. Since the limited number of actuators can only correct low-frequency shape errors, the curvature estimator should have the capability of extracting local curvature from measurement data with high-frequency components (*e.g.* the surface roughness and the measurement noise). Three methods are introduced here to complete the curvature estimation.

2.1. Windowed Fourier ridges

The first method, 'windowed Fourier ridges' (WFR), was originally proposed for fringe analysis (Kemao, 2004; Huang *et al.*, 2010). The WFR method has the capability of calculating the local angular frequency, which is the first derivative of the fringe phase. If we consider the slope data as the fringe phase, the one-dimensional (1-D) WFR method can provide the curvature (the first derivative of slope). In implementation, we construct a 1-D plural fringe $f(x)$ which can be described as

$$f(x) = \exp[is(x)], \quad (4)$$

where $\exp[\ldots]$ is the exponential function, $s(x)$ stands for the measured slope, and i is the imaginary unit with $i^2 = -1$. The 1-D WFR can be presented as

$$Sf(u, \xi) = \int_{-\infty}^{\infty} f(x)\, g(x - u) \exp(-i\xi x)\, dx, \quad (5)$$

where $Sf(u, \xi)$ is the two-dimensional spectrum for 1-D WFR, x and u are spatial coordinates, ξ is the angular frequency, and the window function $g(x)$ is usually chosen to be a normalized Gaussian function for $\|g(x)\|_2 = 1$ as

$$g(x) = \frac{1}{\sqrt{\sqrt{\pi}\sigma}} \exp\left(-\frac{x^2}{2\sigma^2}\right), \quad (6)$$

where σ is the standard deviation. The local angular frequencies ω at position u can be expressed as

$$\omega(u) = \arg\max_{\xi} \left|Sf(u, \xi)\right|. \quad (7)$$

As a result, the first derivative of the slope, or the curvature C, can be determined as

$$C = \omega/\Delta x, \quad (8)$$

where Δx stands for the spatial sampling step in the x-direction. Fig. 2 demonstrates that the first derivative of a given 1-D data set can be calculated using the 1-D WFR method. The grayscale in the bottom image in Fig. 2 shows the amplitude of

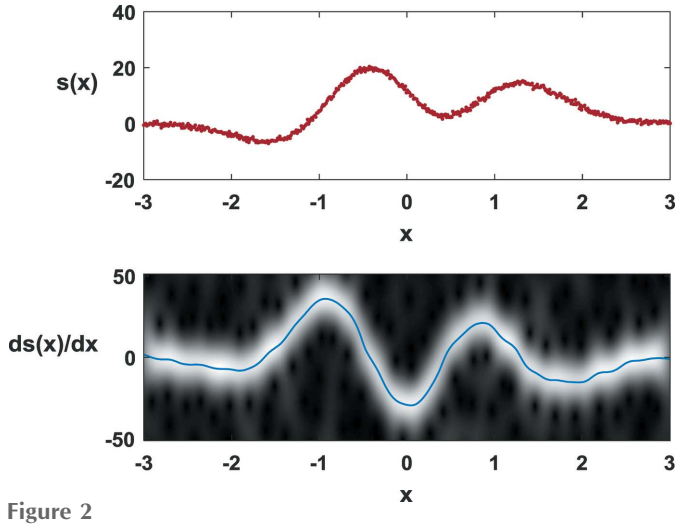

Figure 2
The WFR method can estimate the first derivative of given slope data.

Sf, and its maxima along the x-direction are called the 'ridge'. The values of the first derivative are achieved at the ridges for each lateral coordinate.

An interpolation procedure may be required to obtain the curvature values at the actuator locations. In practice, the locations where the actuators are installed can be known from the mechanical design of the XDM.

2.2. Weighted polynomial fitting

Another method is the 'weighted polynomial fitting' (WPF). Similar to the WFR method, a window centred at the actuator location is used to select the data for analysis as shown in Fig. 3.

Only the slope data inside the window region are analysed. The windowed data are then fitted with polynomials (usually no more than seven orders to avoid overfitting), see equation (9),

$$\frac{dz}{dx} \hat{=} s(x) = \sum_{n=0}^{N} p_n x^n. \quad (9)$$

Once the polynomial coefficients p_n are determined by the least-squares method, the first derivative can be expressed in a form of polynomials,

$$C(x) \approx \frac{d^2z}{dx^2} \hat{=} \frac{ds(x)}{dx} = \sum_{n=1}^{N} p_n n x^{n-1}. \quad (10)$$

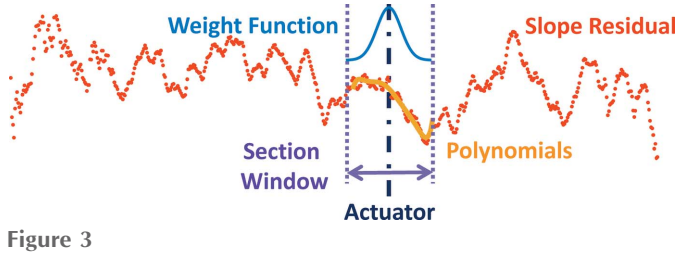

Figure 3
The measured slope can be fitted with polynomials section by section, and the curvature is then represented through the determined polynomial coefficients.

Finally, a weight function (commonly a normalized Gaussian function) is applied when averaging the curvature results within a section to enhance the noise resistance of the method.

2.3. B-spline based method

Instead of using window-based methods, we can use B-splines (Unser *et al.*, 1993) to estimate curvature values from the measured slopes in order to achieve automatic data analysis. In particular, we can represent the slope data with a uniform cubic B-spline (UCBS) as

$$\frac{\mathrm{d}z}{\mathrm{d}x} \triangleq s(x) = \sum_{j=1}^{J} c_j N_j(x), \tag{11}$$

where $N_j(x)$ is the UCBS basis function which is fully determined with a known sampling position x, and the coefficients c_j are estimated in a least-squares sense with the measured slope data. It is straightforward to calculate the derivative with B-splines as demonstrated in Fig. 4, because the derivative of a B-spline of degree d can be expressed as a linear combination of B-splines of degree $d-1$,

$$\frac{\mathrm{d}N_{j,d+1}(x)}{\mathrm{d}x} = d\left(\frac{N_{j,d}(x)}{k_{j+d}-k_j} - \frac{N_{j+1,d}(x)}{k_{j+d+1}-k_{j+1}}\right), \tag{12}$$

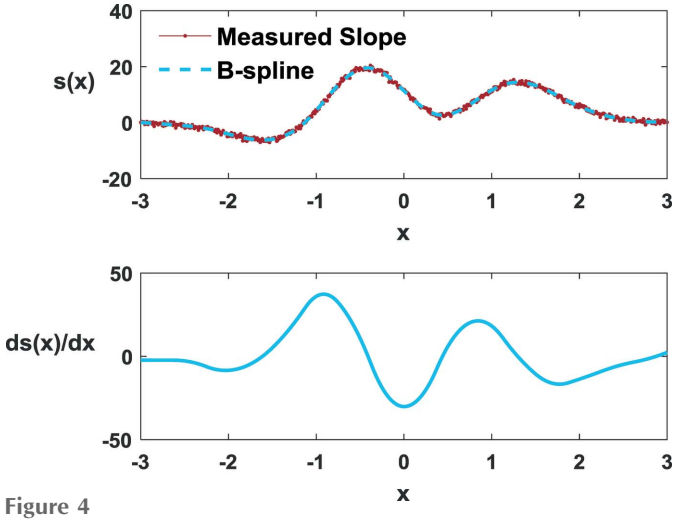

Figure 4
B-splines can fit the measured slope and estimate its derivative as well.

where $k_j \le k_{j+1} \le \ldots \le k_{j+d} \le k_{j+d+1}$ are the selected knots. Therefore, the curvature can be expressed as

$$C(x) \approx \frac{\mathrm{d}^2 z}{\mathrm{d}x^2} \triangleq \frac{\mathrm{d}s(x)}{\mathrm{d}x} = \sum_{j=1}^{J} c_j \frac{\mathrm{d}N_{j,d+1}(x)}{\mathrm{d}x}. \tag{13}$$

Once the curvature C has been estimated, the voltages can be accordingly updated for the next iteration, if necessary. In the next section, we will demonstrate several experiments to show the feasibility of the iterative approach. The three proposed methods for curvature estimation are used in these mirror inspection experiments.

3. Experiments

In this section we show a series of experiments where a Stitching Shack–Hartmann (SSH) metrology system (Idir *et al.*, 2014) is used to control and inspect the XDMs towards target shapes (see Fig. 5).

In the first series of experiments the curvatures are then estimated using the WFR method from the slope data taken with the SSH. In the second experiment the WPF method is employed, and the B-spline method is applied in the third experiment.

3.1. Experiment using the WFR method

In the first experiment, the XDM under test is a 700 mm-long bimorph mirror with 12 actuators. There are two target ellipses for this piece of XDM. The first ellipse parameters are $p = 37.35$ m, $q = 13.65$ m, $\theta = 3.5$ mrad, and the parameters for the second are $p = 37.35$ m, $q = 22.65$ m, $\theta = 3.5$ mrad. The starting voltages for the first ellipse ($p = 37.35$ m, $q = 13.65$ m, $\theta = 3.5$ mrad) are suggested by the XDM fabricator. However, maybe due to mirror transportation and the difference in measurement conditions, the suggested voltages do not drive the mirror to the target shape with the expected specified value of 0.5 µrad r.m.s., whereas it is still a good initial point to start the iteration.

The slope of the mirror is measured by SSH after voltages are applied. Comparing the current slope with the target one, the slope residual is 1.03 µrad r.m.s. as plotted in Fig. 6. Using the WFR method, the curvature residual can be estimated. The suggested voltages in Fig. 6 are calculated with the value

Figure 5
XDMs are inspected with our stitching Shack–Hartmann system in the NSLS-II metrology laboratory.

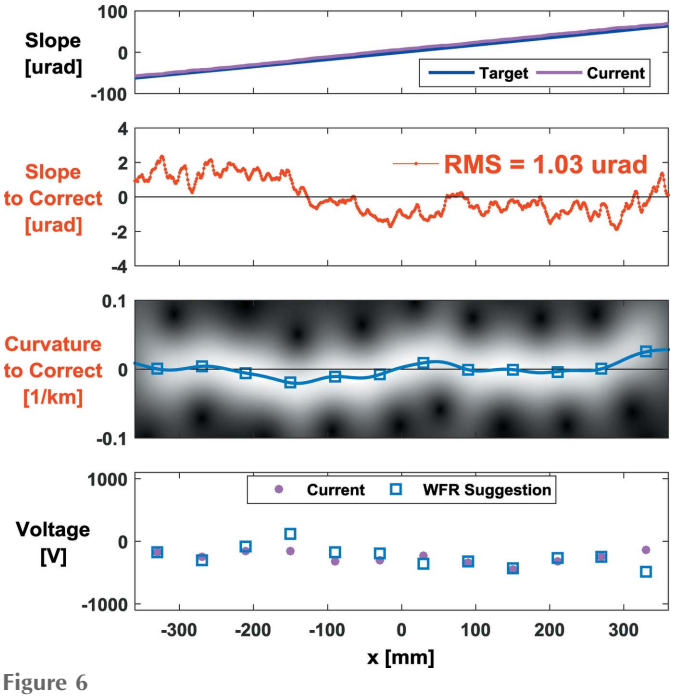

Figure 6
Voltages are suggested by calculating the curvature residuals using the WFR method.

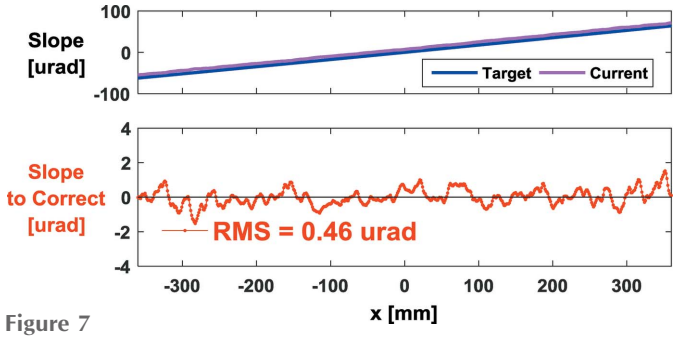

Figure 7
The second mirror iteration gives smaller slope residuals.

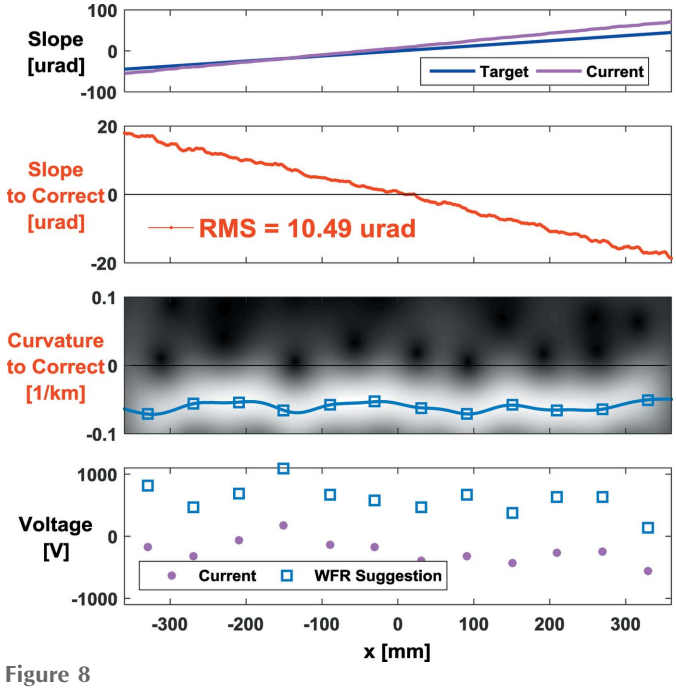

Figure 8
Curvature needs to be changed accordingly, once the target changes.

of K that is also provided by the XDM fabricator and then updated to the XDM for the next measurement. Fig. 7 shows that the slope residuals are reduced to 0.46 µrad r.m.s. after applying the suggested voltages, which indicates that the feedback is effective. The 0.46 µrad r.m.s. slope error converted to height profile error is about 15.1 nm r.m.s. and 67.1 nm peak-to-valley (PV).

It is possible to continue driving the mirror from the present shape to the second target ellipse (p = 37.35 m, q = 22.65 m, θ = 3.5 mrad). As shown in Fig. 8, it is obvious that the slope residual will be rather large (10.49 µrad r.m.s.) once we change the target shape from the first ellipse to the second one.

The curvature residual estimated with the WFR method in Fig. 8 indicates a large curvature variation along the full mirror size due to the modification of the target. The voltage change calculated from equation (1) is used as feedback in the loop. The suggested voltages shown in Fig. 8 are updated to deform the mirror and the iteration continues.

Fig. 9 shows that the iterations can effectively reduce the root mean square error (RMSE) of the updated slope data. With two more iterations, the RMS of slope residuals was successfully reduced from 10.49 µrad to 0.43 µrad as shown in Fig. 9, which is already similar to the performance for the first ellipse

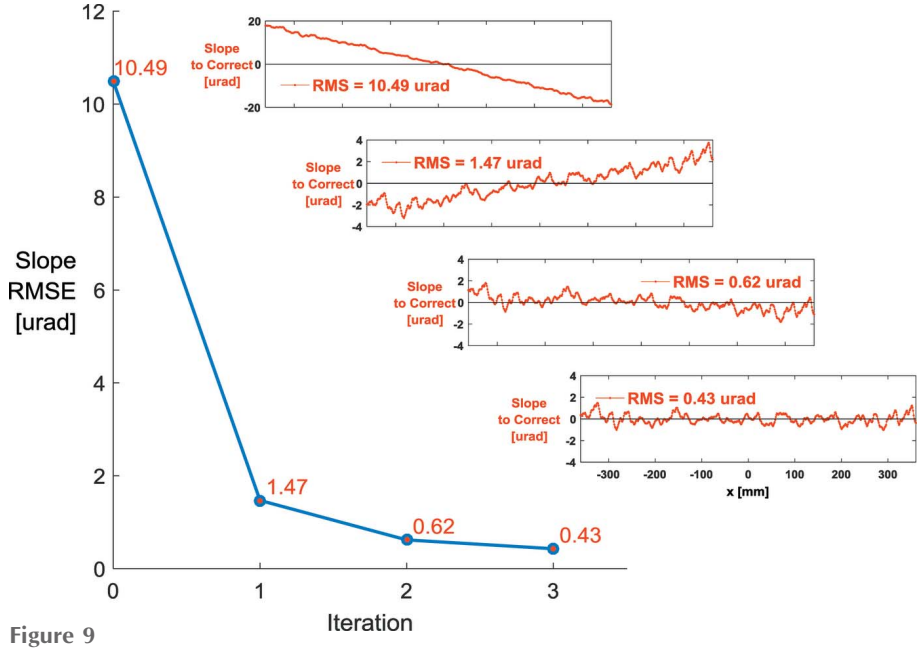

Figure 9
Slope residuals reduce along iterations. The slope residual drops from 10.49 µrad r.m.s. to less than 0.5 µrad r.m.s. with three iterations.

target shown in Fig. 7. The 0.43 µrad r.m.s. slope error converted to height profile error is about 12.6 nm r.m.s. and 50.6 nm PV. The results in Figs. 7 and 9 indicate that the WFR method can successfully calculate the curvature from the measured slope data and provide the correct feedback to guide the mirror towards the targets.

3.2. Experiment using the WPF method

In this section, we demonstrate another experiment of controlling an XDM to show the effectiveness of the proposed approach with the WPF curvature estimator. The bimorph mirror under test is about 740 mm long with 16 actuators and two 4 mm-wide stripes (Pd-coating and Si). The Shack–Hartmann optical head used as a metrology tool has about a 12 mm × 18 mm field of view in a single shot, so both stripes can be measured during one scan. The target shape for both stripes is the same ellipse with p = 40.69 m, q = 11 m, θ = 2.5 mrad with 0.2 µrad r.m.s. residual slope error.

Starting with the fabricator-suggested voltages, the Pd-coating stripe is analysed first and the RMSE of the slope is about 0.33 µrad. With a polynomial fitting section by section, the coefficients of polynomials are determined to represent the slope data as shown in Fig. 10.

In addition, the curvature values at the 16 actuator locations can be estimated through the determined polynomial coefficients according to equation (10). The voltage updates are then determined and applied to the XDM for the next round of metrology.

Fig. 11 shows that the slope is reduced to 0.21 µrad r.m.s. in two iterations. The 0.21 µrad r.m.s. slope error converted to height profile error is about 4.4 nm r.m.s. and 17.4 nm PV. It is not difficult to notice that the slope residuals seem quite similar to each other during the optimization, except for the changes of the local curvature (local tilts in slope).

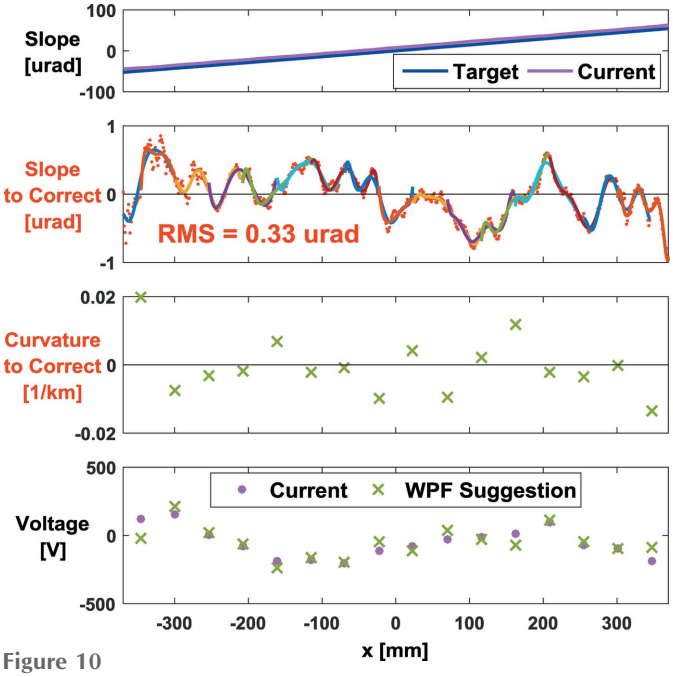

Figure 10
Voltages are updated with WPF-estimated curvatures.

If we move our analysis to the Si stripe, due to the difference in location of the stripes in the mirror, the optimized voltages used for the Pd-coating stripe will not work perfectly (see Fig. 12; the Si strip is at 0.43 µrad r.m.s. with the same

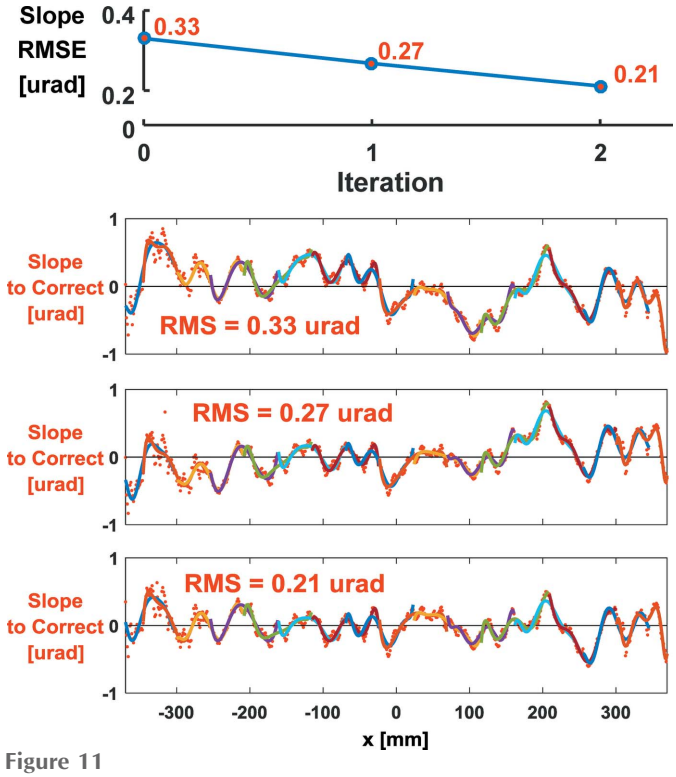

Figure 11
Curvature estimation using the WPF method guides the slope error on the Pd-coating stripe down to a lower level.

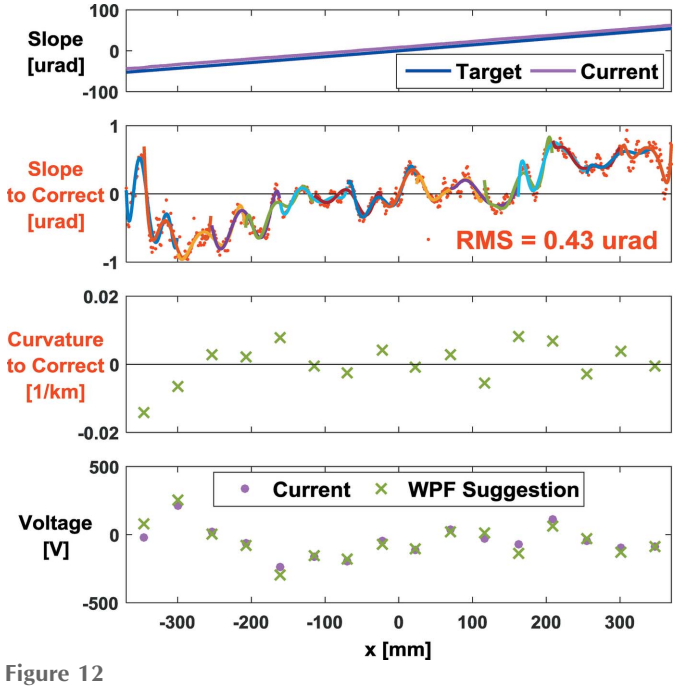

Figure 12
Optimal voltages found for the Pd-coating stripe do not provide the same level of slope error on the Si stripe. Additional iterations are needed to obtain the optimal voltages for the Si stripe.

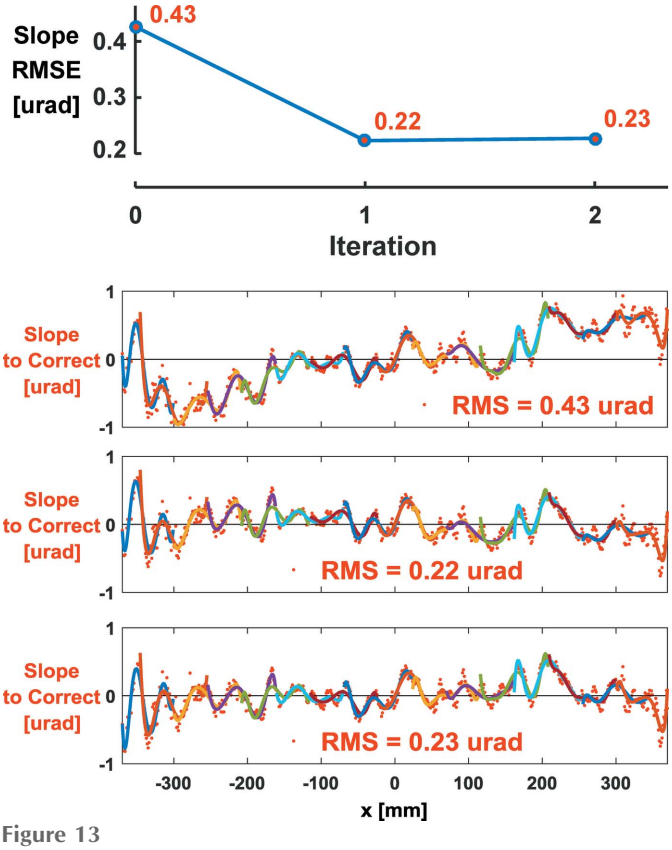

Figure 13
The Si stripe is investigated from the optimal voltages for the Pd-coating stripe, and it converges to 0.23 µrad r.m.s.

target ellipse). In order to find the optimal voltages for the Si stripe, an additional iteration needs to be performed.

One of the advantages of the proposed method is that the initial voltages for a new loop can be any applicable voltages (satisfying the voltage constrains), which means the iteration for the Si stripe can start from the optimized voltages for the Pd-coating stripe.

After one iteration, the slope error for the Si stripe is reduced to 0.22 µrad r.m.s. (see Fig. 13), which is close to the result of the Pd-coating stripe. Just to be sure whether there is some room to improve the shape, one more round is conducted. The resultant slope residuals become 0.23 µrad r.m.s. (see the last iteration in Fig. 13). The 0.23 µrad r.m.s. slope error converted to height profile error is about 10.1 nm r.m.s. and 35.3 nm PV. Comparing with the previous round, the RMS of the slope residuals keeps at the same level with no obvious improvement and the slope variation is less than our measurement uncertainty, which indicates that it could be treated as the optimized status for this XDM under investigation with the particular metrology, mirror surface and degree of freedom by these actuators.

3.3. Experiment using the B-spline method

In this section we demonstrate that the B-spline based method can be used to estimate the curvatures and then feedback voltages to control the XDM towards the right target from all-zero voltages as our starting point. In this experiment

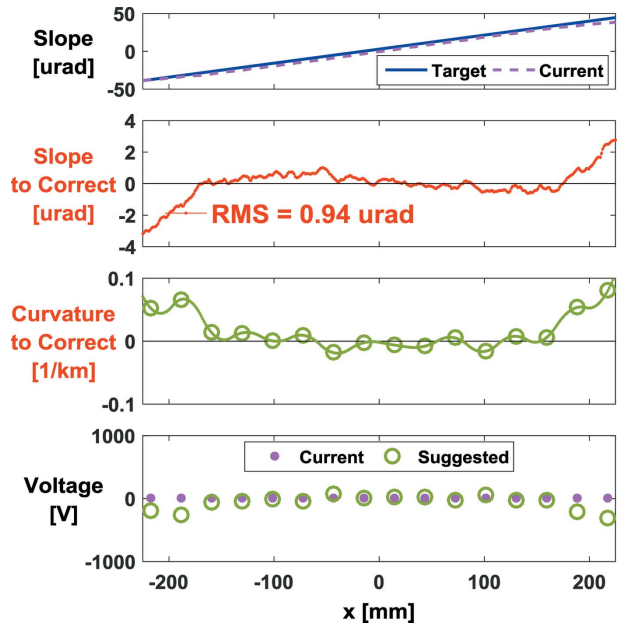

Figure 14
Voltage updates are suggested *via* the curvature estimation using the B-spline method.

the XDM under test is a 500 mm-long bimorph mirror with N = 16 actuators. The target shape is a cylinder with a radius of curvature R = 5390 m.

As shown in Fig. 14, starting with all actuators at zero volts, the measurement shows that the mirror slope error is 0.94 µrad r.m.s. from the cylinder target. By using the B-spline to estimate the 'curvature distance' using as a break number the actuator number N = 16, a new voltage combination is suggested.

The suggested voltages in Fig. 14 are then updated to the XDM for the next iteration. Fig. 15 shows that the slope residuals drop down to 0.27 µrad r.m.s. after applying the suggested new voltages, which indicates that the iteration process is effective. A fine adjustment on voltages is suggested from B-spline based curvature analysis.

By using the newly updated voltages, the residual slope error further reduces to 0.19 µrad r.m.s. after one more round as shown in Fig. 16. Since the slope residual meets the specification (<0.2 µrad r.m.s.), the iteration stops. The 0.19 µrad r.m.s. slope error converted to height profile error is about 4.5 nm r.m.s. and 17.8 nm PV.

Fig. 17 shows that the iterations can effectively reduce the RMSE of the updated slope data. With two iterations, the slope residuals are reduced from 0.94 µrad r.m.s. to 0.19 µrad r.m.s. The results indicate that the B-spline based method successfully estimates the curvature from the measured slope data and offers the correct feedback to control the mirror towards the target shape.

4. Discussion

It is meaningful to discuss the limitations and merits of the proposed approach with the three derivative estimators to

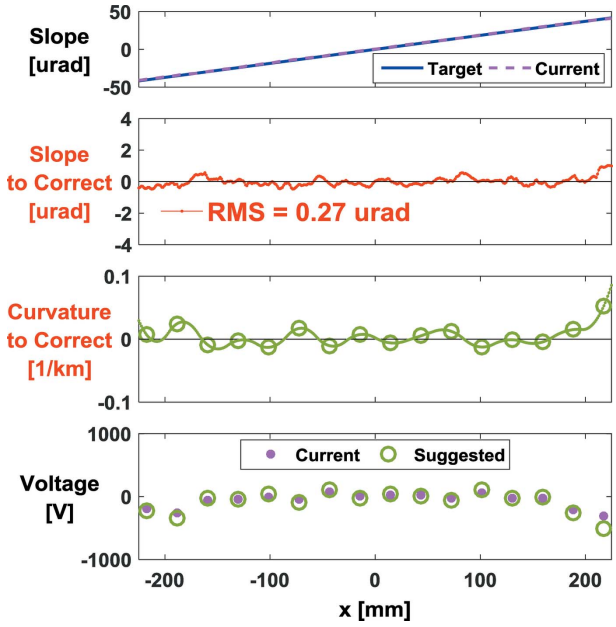

Figure 15
The mirror with updated voltages has smaller slope residuals.

identify some potential improvements. Generally speaking, the proposed approach has the following limitations and merits.

Limitations:

(i) This approach can inspect the XDM for quality check, but it is not able to predict voltages for an arbitrary target shape, since the influence function is not measured.

(ii) The proposed method assumes that all actuators are similar with the same coefficient K. A reliable way to determine the localized parameter K (each actuator may have a different K value) may be needed for further improvement.

Merits:

(i) There is no need to measure all of the influence function for each actuator, which saves metrology time.

(ii) During the iteration, the slope or height is monitored by the metrology tool. The resultant performance under the optimal voltages is always double-checked with measurement.

The three methods for derivative estimation have their advantages and disadvantages as well. The WFR and WPF methods are window-based methods, so the window size becomes a parameter which may need adjustment in handling different XDMs according to different actuator numbers, and mirror length, as well as scanning steps. In addition, the WFR method is not good for calculating the derivatives at the two boundary regions of the mirror, because zero padding at the data

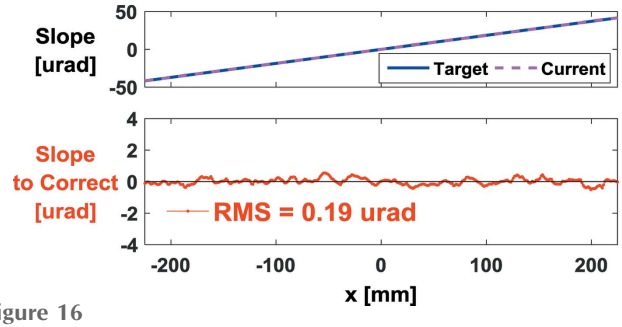

Figure 16
Curvature needs to be changed accordingly, once the target changes.

boundaries will yield error in estimation. In contrast, the data processing with the B-spline based method is highly automatic with no human–computer interaction, so the issue of window size selection in the WFR and WPF methods is avoided in principle, but the WFR and WPF methods are relatively easier to implement.

5. Conclusion

In this work, a practical scheme is presented to control and inspect the XDM with a feedback mechanism. The mirror shape is measured under a closed-loop control by adjusting the applied voltages. By estimating the curvature residual according to the slope or height metrology data, the voltages are updated based on the relation between the changes of voltage and curvature. Three methods (WFR, WPF and B-spline) are introduced to estimate the derivative in order to obtain the curvature from the measured slope or height data. A series of experiments demonstrates that the proposed approach is able to control the XDMs towards the desired

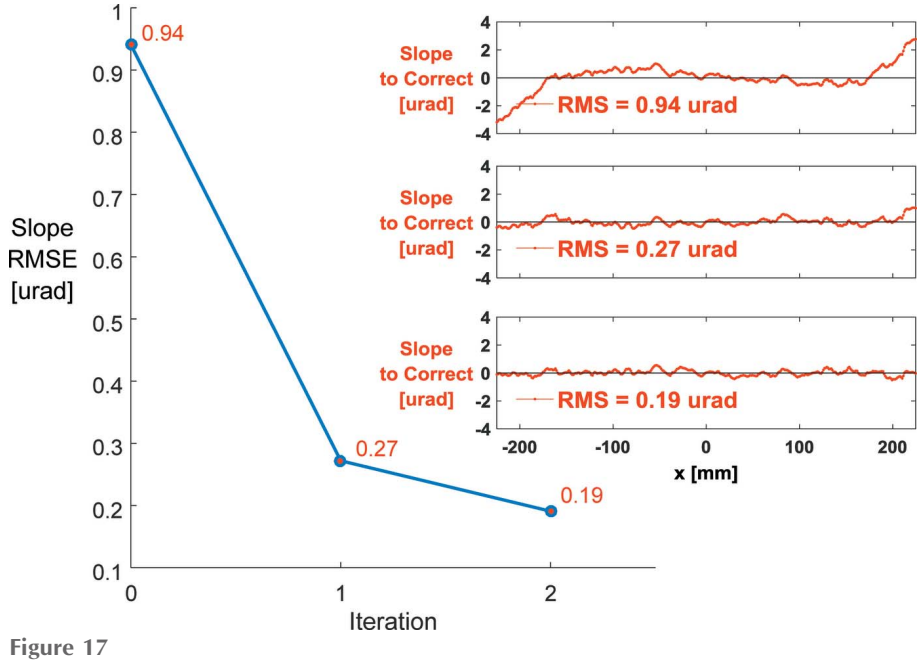

Figure 17
Slope residuals reduce along the iterations. The slope residual reduced from 0.94 µrad r.m.s. to 0.19 µrad r.m.s. with two iterations.

target shapes. The iteration commonly converges with three or four measurements. This technique is effective and efficient in day-to-day XDM inspection in an optical metrology laboratory. It should be noted that this approach can also be used *in situ* with an X-ray wavefront sensor (pencil beam, Hartmann, grating shearing, or curvature sensor).

Acknowledgements

This work was supported by the US Department of Energy, Office of Science, Office of Basic Energy sciences, under contract No.DE-AC-02-98CH10886. We would like to thank Luca Peverini from Thales-SESO for the helpful initial discussion of the proposed method and the NSLS-II ABBIX team and the NSLS-II SMI team for the possibility to use their bimorph mirrors for our project and Guillaume Dovillaire from Imagine Optic for the discussion on the metrology aspect of the bimorph mirrors.

References

Huang, L., Kemao, Q., Pan, B. & Asundi, A. K. (2010). *Opt. Lasers Eng.* **48**, 141–148.
Idir, M., Kaznatcheev, K., Dovillaire, G., Legrand, J. & Rungsawang, R. (2014). *Opt. Express*, **22**, 2770–2781.
Idir, M. & Mercere, P. (2013). *Imaging Appl. Opt.* p. OM3A.1. Arlington: Optical Society of America.
Kemao, Q. (2004). *Appl. Opt.* **43**, 2695–2702.
Qian, S., Jark, W. & Takacs, P. Z. (1995). *Rev. Sci. Instrum.* **66**, 2562–2569.
Siewert, F., Noll, T., Schlegel, T., Zeschke, T. & Lammert, H. (2004). *AIP Conf. Proc.* **705**, 847–850.
Takacs, P. Z., Qian, S. & Colbert, J. (1987). *Proc. SPIE*, **0749**, 59–64.
Tyson, R. K. (2000). *Introduction to Adaptive Optics.* Bellingham: SPIE Press.
Unser, M., Aldroubi, A. & Eden, M. (1993). *IEEE Trans. Signal Process.* **41**, 821–833.
Vannoni, M., Freijo Martín, I., Siewert, F., Signorato, R., Yang, F. & Sinn, H. (2016). *J. Synchrotron Rad.* **23**, 169–175.
Vannoni, M., Yang, F. & Sinn, H. (2015). *Opt. Eng.* **54**, 015104.
Yamauchi, K., Yamamura, K., Mimura, H., Sano, Y., Saito, A., Ueno, K., Endo, K., Souvorov, A., Yabashi, M., Tamasaku, K., Ishikawa, T. & Mori, Y. (2003). *Rev. Sci. Instrum.* **74**, 2894–2898.